Hobbs *et al. - Supporting Information Appendix*

Supporting Information Text

Chemical shifts, coupling constants and assignments for the two observed products of ΔGalA digestion:

4-deoxy-5-hydroxy-α-D-idopyranuronate: 4.66 ppm (1H, d, J = 4 Hz, H-1), 4.02 ppm (1H, ddd, J = 12, 10, 5 Hz, H-3), 3.86 ppm (1H, dd, J = 10, 4 Hz, H-2), 2.49 ppm (1H, dd, J = 14, 5, H-4 equatorial), 1.88 ppm (1H, dd, J = 14, 12 Hz, H-4 axial)

4-deoxy-5-hydroxy-α-D-glucopyranuronate: 4.61 ppm (1H, d, J = 4 Hz, H-1), 3.96 ppm (1H, ddd, J = 8, 8, 5 Hz, H-3), 3.86 ppm (1H, dd, J = 7, 4 Hz, H-2), 2.40 ppm (1H, dd, J = 15, 5 Hz, H-4 equatorial), 2.00 ppm (1H, dd, J = 15, 8 Hz, H-4 axial)

Resonances for H-2, H-3, and H-4ax/eq in each product, and the assignment of ido- vs. gluco-isomeric structures, are assigned based on the expected shifts and coupling constants for these products and are confirmed by comparison to NMR spectra of structurally similar β-anomer isomers of 4-deoxy-5-hydroxy-idopyranuronate and 4-deoxy-5-hydroxy-glucopyranuronate (1). The assignment of both products in the current work as α-anomers is based on the small coupling constants (4 Hz) between H-1 and H-2, consistent with the equatorial-axial coupling expected for α-anomeric products and distinct from the larger axial-axial coupling constants seen in the previously reported β-anomers. See Tables S2 and S3 for complete details.

Supporting Information Methods

Bacterial Strains, Plasmids and Chemicals

Escherichia coli ATCC 25922 (GenBank accession number ASHD00000000.1) and genomic DNA for *Yersinia enterocolitica subsp. enterocolitica* 8081 (ATCC 9610D; GenBank accession number NC_008800) were both obtained from Cedarlane Laboratories. The plasmids pKOV-unstuff and pET15b-Alg17c were obtained from Prof Benjamin Kerr, University of Washington and Prof Satish Nair, University of Illinois, respectively. Polyuronates were purchased from Sigma-Aldrich (polygalacturonate), Santa Cruz Biotechnology (digalacturonate) and Aglyco (D-dimannuronate).

Isolation, Genome Sequencing and Annotation of *Halomonas sp.*

Halomonas sp. was isolated from *Macrocystis* sp. growing in the intertidal zone near Victoria, British Columbia during spring 2010. A seaweed broth was prepared from 1% (w/v) dried *Fucus* sp. in artificial seawater (Sigma-Aldrich) and sterilized by autoclaving. This broth was then inoculated with fragments of freshly collected, partially decomposed *Macrocystis* sp. and incubated at 20 °C and 200 rpm until dense bacterial growth had occurred (36 hours). The culture was diluted in artificial seawater (ASW) medium and streaked on seaweed broth agar plates. Single white colonies were re-streaked twice to ensure purity. Isolated colonies were further screened for their ability to use alginate as the sole carbon source by plating on minimal marine medium (2) containing 0.25% (w/v) agarose and vitamin mix (3). Genomic DNA extractions were performed using the QIAamp DNA mini kit (Qiagen) after culture of bacteria in marine broth 2216 (Difco) at 20 °C and 200 rpm for 24 hours. Genome sequencing was performed by the Genome Sciences Centre of the British Columbia Cancer Agency. Briefly, the purity, quality and quantity of DNA was analyzed using an Agilent Bioanalyzer, and 1 µg was used for library preparation for Illumina PET sequencing. Genome assembly was performed using the default parameters of ABySS 1.3.4. An assembly was run at every 8 k value from 56 to 96 with the 96 k assembly selected as the best on the basis of an optimized N50 value. 4.37 mega base pairs of sequence were assembled in 68 contigs larger than 200 base pairs, with 50% of the genome assembled in 5 contigs larger than 246 kilo base pairs. The largest contig was 690 kilo base pairs. Open reading frames were identified and annotated using the automated RAST annotation pipeline (4). The nucleotide sequence of *kdgF* from *Halomonas* sp. is available from GenBank under accession number KU156827; the remaining genes in the *kdgF* operon are available under the accession numbers KU697803-KU697810.

Cloning and Mutagenesis

The generation of the expression constructs pET28a-*Ye*OgI and pET28a-*Ye*PL2A has been described previously (5, 6). The genes encoding for *Ye*KdgF (locus tag YE1889) and *Ha*KdgF were amplified from genomic DNA using the primers *Ye*KdgF fwd/rev and *Ha*KdgF fwd/rev (Table S5), respectively, and ligated into pET28a between the *Nhe*I and *Xho*I restriction sites. The genes encoding for *Ec*KdgF (K758_20431), *Ye*KduI (YE1888) and *Ye*KduD (YE1887) were amplified and cloned into pET28a using the In-Fusion HD Cloning Kit (Clontech Laboratories Inc.) and the primers *Ec*KdgF fwd/rev, *Ye*KduI fwd/rev and *Ye*KduD fwd/rev (Table S5), respectively. The same kit, combined with mutagenic primers (Integrated DNA Technologies), was used to introduce mutations into pET28a-*Ye*KdgF. All cloning and mutagenesis was confirmed by sequencing (Sequetech Corp.).

Protein Expression and Purification

All proteins, with the exception of Alg17c, were expressed in BL21(DE3) in Luria-Bertani (LB) broth at 16 °C for 18 hours with 0.5 mM IPTG induction. Alg17c was expressed in Rosetta as previously described (7). Recombinant proteins were released from cells by chemical lysis and purified by immobilized Ni^{2+}-affinity chromatography in binding buffer (20 mM Tris-HCl pH 8.0, 500 mM NaCl) with an imidazole gradient. All proteins were dialyzed against 20 mM Tris-HCl pH 8.0 overnight at 4 °C prior to use, with the exception of Alg17c which was dialyzed against 50 mM Tris-HCl pH 7.5, 100 mM NaCl. *Ye*KdgF and *Ha*KdgF were further purified prior to crystallization by size-exclusion chromatography using a HiPrep 16/60 Sephacryl S-100 HR column (GE Healthcare) equilibrated with 20 mM Tris-HCl pH 8.0. All proteins were concentrated at 4°C using an Amicon stirred ultrafiltration unit fitted with either a 5 or 10 kDa molecular weight cut-off cellulose membrane as appropriate. The purity of all proteins was assessed by SDS-PAGE.

Enzyme Assays

The concentration-dependent activity of *Ye*kdgF and *Ec*KdgF on unsaturated galacturonate was determined in a linked assay with *Ye*Ogl. Digalacturonate at 1 mM was prepared in assay buffer (100 mM Tris-HCl pH 7.5) and incubated with 0.5 µM *Ye*Ogl at 25 °C. The production of unsaturated galacturonate was monitored at 230 nm in a SpectraMax M5 plate reader (Molecular Devices) using a UV-Star® 96-well microplate (Greiner Bio-One) as previously described (6). Once the absorbance had plateaued, *Ye*KdgF or *Ec*KdgF were added at different concentrations and the decrease in absorbance followed (an equivalent volume of 20 mM Tris-HCl pH 8.0 was added to the 0 nM KdgF reactions). The concentration-dependent activity of *Ha*KdgF on unsaturated mannuronate was determined in the same manner but employed Alg17c at 0.23 µM in place of *Ye*Ogl. Absorbances at 230 nm were converted to µM using an extinction coefficient of 5200 M^{-1} cm^{-1} (8). For substrate specificity assays, *Ye*KdgF and *Ha*KdgF were used at 1 µM. The activities of *Ye*KdgF mutants at 250 nM were determined as described above and compared with wildtype *Ye*KdgF. Wildtype *Ye*KdgF was always tested alongside the mutants and used for relative activity calculations to account for any plate-specific variance. The rate for each enzyme was determined from the first 1-3 minutes of data and corrected for any activity observed in the absence of *Ye*KdgF. Metal dependence assays were performed with *Ye*KdgF that had been treated with 50 mM EDTA and then dialyzed overnight against 20 mM Tris-HCl pH 8.0 (previously treated with Chelex resin to remove metals) containing 2 mM of different metals (or no metal) (9). The initial rate of activity was determined as described for mutant enzymes. A second linked assay was established in which the oxidation of NADH was

used as a read-out of sequential digalacturonate processing by *Ye*Ogl, *Ye*KdgF, *Ye*KduI and *Ye*KduD. Reactions containing 200 µM NADH and different combinations of *Ye*Ogl, *Ye*KdgF, *Ye*KduI and *Ye*KduD at 0.5 µM each were set up in assay buffer at 25 °C and initiated with the addition of digalacturonate to 1 mM. The activity of *Ye*KduD was followed as a decrease in absorbance at 340 nm and the absorbance values converted to µM of NADH oxidized using an extinction coefficient of 5200 M^{-1} cm^{-1}. All enzyme assay data were processed, and statistical analyses performed, using GraphPad Prism 6.0.7.

Differential Scanning Fluorimetry

Thermal unfolding curves for *Ye*KdgF and its mutants were generated using the fluorophore SYPRO® Orange (Life Technologies) in a Bio-Rad CFX96 Touch™ real-time PCR machine as previously described (10). Proteins (1 mg/ml final) were unfolded in 50 mM Tris-HCl pH 7.5 with SYPRO® Orange at a final concentration of 10× and a ramp rate of 1 °C/minute.

Crystallization and Structure Determination

*Ye*KdgF and *Ha*KdgF were crystallized using the hanging drop vapor diffusion method at 18 °C. Crystals of *Ye*KdgF in the spacegroup $P2_12_12_1$ were obtained in 0.1 M CAPSO pH 9.0, 21% PEG 3350, 0.28 M $MgCl_2.6H_2O$ with protein at 20 mg/ml and cryoprotected in crystallization solution supplemented with 20% ethylene glycol. Crystals of *Ye*KdgF in the spacegroup $P3_221$ were obtained in 75% tacsimate pH 7.0 with protein at 25 mg/ml and cryoprotected with 75% tacsimate. Crystals of *Ha*KdgF were obtained in 20 mM Tris-HCl pH 7.5, 1.2 M sodium citrate with protein at 20 mg/ml and cryoprotected in crystallization solution supplemented with 20% ethylene glycol. Crystals were flash-cooled in liquid nitrogen and kept at 113K for diffraction data collection. Diffraction data were collected at the University of Victoria at a wavelength of 1.54187 Å using a Rigaku R-AXIS IV++ area detector coupled to a MM-002 X-ray generator with Osmic “blue” optics and an Oxford Cryostream 700, or at the Canadian Light Source on beamline 08ID-1. Diffraction data were integrated with Mosflm (11), and scaled and merged using SCALA (12, 13). The structure of *Ye*KdgF in P212121 spacegroup was solved by molecular replacement using an RmlC-like cupin from *Shewanella frigidimarina* (PDB ID code 2PFW) as a search model and the program PHASER (14). Starting with this model, ARP/wARP (15) was used to build a nearly complete model of *Ye*KdgF, which was finished by iterative manual building with COOT (16) and refinement with REFMAC (17). A monomer from this *Ye*KdgF model was used as a search model to solve the structures of *Ha*KdgF and *Ye*KdgF in the $P3_221$ spacegroup. Again, model completion was achieved by iterative manual building with COOT and refinement with REFMAC. All data collection and processing statistics are shown in

Table S4. For all structures, the addition of water molecules was performed in COOT with FINDWATERS and manually checked after refinement. In all data sets, refinement procedures were monitored by flagging 5% of all observations as ‘‘free’’ (18). Model validation was performed with MOLPROBITY (19).

Preparation and Purification of 4,5-Unsaturated Digalacturonate ($\Delta GalUA_2$)

$\Delta GalUA_2$ was prepared by digesting polygalacturonic acid (Sigma P-1879) with the endolytic pectate lyase *Vv*PL2 (9). Digestions consisting of 1 µM *Vv*PL2, 50 mM CAPSO pH 9.0, 1 mM $MgCl_2$ and 1 mg/ml polygalacturonic acid were incubated at 37ºC overnight, and the subsequent products separated on a Bio-Gel P2 size-exclusion column (Bio-Rad) running at 0.25 ml/min for 35 hours. Fractions containing $\Delta GalUA_2$ were identified by thin layer chromatography as previously described (9), pooled and lyophilized.

^{1}H NMR on Digests of $\Delta GalUA_2$

^{1}H NMR spectra were recorded on a Bruker AV-500 spectrometer operating at 500.27 MHz, using an inverse-configuration 5-mm probe with a Z-gradient. Full spectra were obtained with a double pre-saturation to eliminate the water and Tris-HCl resonances at 4.8 and 3.7 ppm, respectively. The spectral width was 16 ppm, with 32K data points, and a relaxation delay of 2 s. A solution of 1 mM $\Delta GalUA_2$ in 100 mM Tris-HCl pH 7.5 was deuterated by the addition of D_2O to 10% (v/v) final. Full spectra were collected of the disaccharide and at regular intervals following the addition of *Ye*KdgF and/or *Ye*Ogl (both at 1 µM final). When the spectra stabilized, indicating that the reactions had reached completion, 1D selective TOCSY sub-spectra were obtained. These spectra were obtained with a Gaussian shaped selective pulse of 36-50 ms centered on one of the geminal pairs at the 4 position and a 120 ms TOCSY spinlock, with the same relaxation delay and resolution as the full spectra. All spectra were run at 300 K. Spectra were referenced to the methyl resonance of sodium 3-trimethylsilylpropionate-2,2,3,3-d_4 (TSP) at 0 ppm by adding a small amount to one of the samples after the spectra had been obtained. This spectral reference setting was transferred to all other spectra.

***kdgF* Deletion and Complementation**

Marker-less deletion of *kdgF* and from the chromosome of ATCC 25922 was performed using a modified version of the vector pKOV (20) in which a stuffer region has been removed (21). Regions of approximately 850 bp immediately upstream and downstream of *EckdgF* were amplified using the primers *kdgF* upstream fwd/rev and *kdgF* downstream fwd/rev (Table S5). The two flanks were joined together and cloned into the modified pKOV vector between the *Not*I and *Bam*HI sites in a single step using the In-Fusion HD Cloning Kit. This construct was then

transformed into ATCC 25922 at 30 °C, a single colony picked and grown in LB broth with 50 µg/ml chloramphenicol at 43 °C overnight to force integration and then plated on LB agar containing chloramphenicol at 43 °C. To excise the plasmid from the chromosome, 4-6 integrant colonies were used to inoculate a single LB culture containing no chloramphenicol which was grown overnight at 30 °C prior to plating on NaCl-free LB agar containing 10% sucrose. Resultant colonies were screened for chloramphenicol sensitivity by replica plating, and chloramphenicol sensitive, sucrose resistant colonies were screened by colony PCR for the presence of *kdgF*. Deletion of *kdgF*, and non-disturbance of the surrounding sequence, was confirmed by amplification with the primers *kdgF* flank fwd/rev (which are positioned outside of the originally amplified upstream and downstream regions) and sequencing of the entire region. Complementation of Δ*kdgF* was achieved in two ways: firstly, the methods described above for deletion of *kdgF* were employed to reinsert *kdgF* into the chromosome (using the primers *kdgF* upstream fwd and *kdgF* downstream rev to amplify the *kdgF*-containing region for cloning), and secondly, *kdgF* was cloned into the low copy number, *tac*-driven vector pGEX-5X-2 (GE Healthcare) using the In-Fusion HD Cloning Kit and the primers pGEX-*kdgF* fwd/rev, which removed the GST fusion tag. The construct pGEX-*kdgF* was then transformed into the Δ*kdgF* strain.

Growth Assay on Polygalacturonate

Strains grown overnight in M9 minimal medium containing 0.4% (w/v) autoclaved PGA, trace metal mix and 0.5 µM filter-sterilized *Ye*PL2A were used to inoculate growth assay cultures in Erlenmeyer flasks. For strains carrying pGEX constructs, ampicillin (100 µg/ml final) and IPTG (0.1 mM final) were also added to the medium. Four replicates were set up for each strain (using four separate overnight cultures), at 37 °C with shaking and samples taken for OD_{600nm} readings every 45-100 minutes. Growth rates and lag times were calculated using the program GrowthRates (22). Statistical analysis was performed in GraphPad Prism 6.0.7.

Supporting Information References

1. Jongkees SA, Withers SG (2011) Glycoside cleavage by a new mechanism in unsaturated glucuronyl hyrolases. *J Am Chem Soc* 133(48):19334-19337.
2. Therkildsen M, Isaksen M, Lomstein B (1997) Urea production by the marine bacteria *Delaya venusta* and *Pseudomonas stutzeri* grown in a minimal medium. *Aquat Microb Ecol* 13(2):213–217.
3. Finster K, Tanimoto Y, Bak F (1992) Fermentation of methanethiol and dimethylsulfide by

a newly isolated methanogenic bacterium. *Arch Microbiol* 157(5):425–430.

4. Overbeek R, et al. (2014) The SEED and the Rapid Annotation of microbial genomes using Subsystems Technology (RAST). *Nucleic Acids Res* 42:D206–14.
5. Abbott DW, Boraston AB (2007) A family 2 pectate lyase displays a rare fold and transition metal-assisted β-elimination. *J Biol Chem* 282(48):35328–36.
6. Abbott DW, Gilbert HJ, Boraston AB (2010) The active site of oligogalacturonate lyase provides unique insights into cytoplasmic oligogalacturonate β-elimination. *J Biol Chem* 285(50):39029–38.
7. Park D, Jagtap S, Nair SK (2014) Structure of a PL17 family alginate lyase demonstrates functional similarities among exotype depolymerases. *J Biol Chem* 289(12):8645–8655.
8. Extinction coefficient
9. McLean R, et al. (2015) Functional analyses of resurrected and contemporary enzymes illuminate an evolutionary path for the emergence of exolysis in polysaccharide lyase family 2. *J Biol Chem* 290(35):21231–43.
10. Niesen FH, Berglund H, Vedadi M (2007) The use of differential scanning fluorimetry to detect ligand interactions that promote protein stability. *Nat Protoc* 2(9):2212–21.
11. Battye TGG, Kontogiannis L, Johnson O, Powell HR, Leslie AGW (2011) iMOSFLM: a new graphical interface for diffraction-image processing with MOSFLM. *Acta Crystallogr D Biol Crystallogr* 67(Pt 4):271–81.
12. Evans P (2006) Scaling and assessment of data quality. *Acta Crystallogr D Biol Crystallogr* 62(Pt 1):72–82.
13. Winn MD, et al. (2011) Overview of the CCP4 suite and current developments. *Acta Crystallogr D Biol Crystallogr* 67(Pt 4):235–42.
14. McCoy AJ, et al. (2007) Phaser crystallographic software. *J Appl Crystallogr* 40(Pt 4):658–674.
15. Langer G, Cohen SX, Lamzin VS, Perrakis A (2008) Automated macromolecular model building for X-ray crystallography using ARP/wARP version 7. *Nat Protoc* 3(7):1171–9.
16. Emsley P, Cowtan K (2004) Coot: model-building tools for molecular graphics. *Acta Crystallogr D Biol Crystallogr* 60(Pt 12 Pt 1):2126–32.
17. Murshudov GN, et al. (2011) REFMAC5 for the refinement of macromolecular crystal structures. *Acta Crystallogr D Biol Crystallogr* 67(Pt 4):355–67.
18. Brünger AT (1992) Free R value: a novel statistical quantity for assessing the accuracy of crystal structures. *Nature* 355(6359):472–475.
19. Chen VB, et al. (2010) MolProbity: all-atom structure validation for macromolecular

crystallography. *Acta Crystallogr D Biol Crystallogr* 66(Pt 1):12–21.

20. Link AJ, Phillips D, Church GM (1997) Methods for generating precise deletions and insertions in the genome of wild-type *Escherichia coli*: application to open reading frame characterization. *J Bacteriol* 179(20):6228–37.
21. Lindsey HA, Gallie J, Taylor S, Kerr B (2013) Evolutionary rescue from extinction is contingent on a lower rate of environmental change. *Nature* 494(7438):463–7.
22. Hall BG, Acar H, Nandipati A, Barlow M (2014) Growth rates made easy. *Mol Biol Evol* 31(1):232–8.
23. Rodionov DA, Gelfand MS, Hugouvieux-Cotte-Pattat N (2004) Comparative genomics of the KdgR regulon in *Erwinia chrysanthemi* 3937 and other gamma-proteobacteria. *Microbiology* 150(11):3571–3590.
24. Wargacki a. J, et al. (2012) An engineered microbial platform for direct biofuel production from brown macroalgae. *Science* 335(6066):308–313.
25. Lombard V, Golaconda Ramulu H, Drula E, Coutinho PM, Henrissat B (2014) The carbohydrate-active enzymes database (CAZy) in 2013. *Nucleic Acids Res* 42:D490–5.

Supporting Information Tables

Table S1. Specific activities for *Ye*KdgF and *Ha*KdgF on ΔGalA and ΔManA

Enzyme	**Specific activity (μM min^{-1} $μg^{-1}$) ±SEM**	
	ΔGalA	**ΔManA**
*Ye*KdgF	191.5 ±2.5	52.9 ±4.9
*Ha*KdgF	168.9 ±8.5	33.3 ±3.9

Values shown were calculated from the slopes shown in Fig. S3 (n=3).

Table S2. Chemical shifts, coupling constants and assignments for 4-deoxy-5-hydroxy-α-D-idopyranuronate

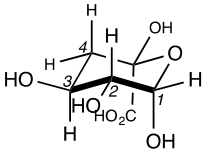

4-deoxy-5-hydroxy-α-D-idopyranuronate

Proton	Chemical shift (type)	Coupling constants and relative geometries
H-1	4.66 ppm (anomeric)	4 Hz (coupled to H-2, equatorial-axial)
H-2	3.86 ppm (CHOH)	4 Hz (coupled to H-1, equatorial-axial) 10 Hz (coupled to H-3, axial-axial)
H-3	4.02 ppm (CHOH)	12 Hz (coupled to H-4, axial-axial) 10 Hz (coupled to H-2, axial-axial) 5 Hz (coupled to H-4, axial-equatorial)
H-4 (equatorial)	2.49 ppm (CH_2)	14 Hz (H-4 — H-4, geminal) 5 Hz (coupled to H-3, equatorial-axial)
H-4 (axial)	1.88 ppm (CH_2)	14 Hz (H-4 — H-4, geminal) 12 Hz (coupled to H-3, axial-axial)

Table S3. Chemical shifts, coupling constants and assignments for 4-deoxy-5-hydroxy-α-D-glucopyranuronate

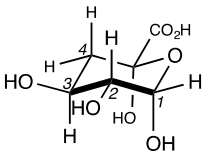

4-deoxy-5-hydroxy-α-D-glucopyranuronate

Proton	Chemical shift (type)	Coupling constants and relative geometries
H-1	4.61 ppm (anomeric)	4 Hz (coupled to H-2, equatorial-axial)
H-2	3.86 ppm (CHOH)	4 Hz (coupled to H-1, equatorial-axial) 7 Hz (coupled to H-3, axial-axial)
H-3	3.96 ppm (CHOH)	8 Hz (coupled to H-4, axial-axial) 8 Hz (coupled to H-2, axial-axial) 5 Hz (coupled to H-4, axial-equatorial)
H-4 (equatorial)	2.40 ppm (CH_2)	15 Hz (H-4 — H-4, geminal) 5 Hz (coupled to H-3, equatorial-axial)
H-4 (axial)	2.00 ppm (CH_2)	15 Hz (H-4 — H-4, geminal) 8 Hz (coupled to H-3, axial-axial)

Table S4. Data collection and refinement statistics

	***Ha*KdgF Citrate**	***Ye*KdgF Malonate**	***Ye*KdgF**
Data collection			
Wavelength (Å)	1.5418	0.979490	0.979490
Space group	C2	$P3_221$	$P2_12_12_1$
Cell dimensions			
a, b, c (Å)	111.29, 78.22, 68.12 (β=113.73°)	60.19, 60.19, 67.83	30.92, 73.76, 83.68
Resolution (Å)	33.2-2.0	52.13-1.5	30-1.5
R_{merge}	0.055 (0.490)	0.057 (0.403)	0.033 (0.436)
R_{pim}	0.041 (0.363)	0.027(0.232)	0.015(0.208)
CC(1/2)	0.998 (0.774)	0.998 (0.839)	1.0 (0.926)
<I/σI>	11.1 (2.0)	13.3 (2.7)	32.2 (3.6)
Completeness (%)	99.9 (89.5)	99.8 (100)	97.3 (78.5)
Redundancy	3.3 (3.0)	4.9 (4.0)	7.2 (6.1)
Total reflections	1180604 (7976)	113049 (13277)	280441 (9360)
Unique reflections	36177 (2646)	23188 (3349)	39140 (1529)
Refinement			
Resolution (Å)	2.0	1.5	1.5
R_{work}/R_{free}	18.5/22.5	17.1/20.5	17.3/19.9
Number of atoms			
Protein	3476	879	1677
Ligand	5 (Ni); 52 (FLC)	7 (MLA); 1 (Ni)	2 (Ni)
Water	281	196	260
B-factors			
Protein	30.9	16.9	20.8
Water	38.6	33.4	36.0
Ligand	27.5 (Ni); 51.3 (FLC)	15.8 (MLA); 11.9 (Ni)	19.8 (Ni)
r.m.s.d.			
Bond lengths (Å)	0.011	0.009	0.0015
Bond angles (°)	1.997	1.417	1.827
Ramachandran (%)			
Preferred	97.0	98.2	98.2
Allowed	3.0	1.8	1.3
Disallowed	0	0	0.5 (1 residue)

Table S5. Oligonucleotide primers used in this study

Primer name	Primer sequence (5'→3')
*Ha*KdgF fwd	CATATC**GCTAGC**AACACAGGCAGTTTCTTC
*Ha*KdgF rev	GGTGGT**CTCGAG**TTATGATTTCAGCATGTCATCGCG
*Ye*KdgF fwd	CATATC**GCTAGC**AAGATGTTCTTTATTAATGATGAAACG
*Ye*KdgF rev	GTGGT**CTCGAG**TTACAAGAAATCATCCCGTTTG
*Ec*KdgF fwd	CGCGGCAGCCATATGTTTGTATTTAATGAAGATACAGC
*Ec*KdgF rev	GGTGGTGGTGCTCGATTACTTTAAAAAATCCTGACGT
*Ye*KduI fwd	CGCGGCAGCCATATGCAAATTTGTCAAAGCATTCATAGC
*Ye*KduI rev	GGTGGTGGTGCTCGATTAGCGCAGTTCGCTAACGG
*Ye*KduD fwd	CGCGGCAGCCATATGATCTTAGATTCCTTTGAGTTAA
*Ye*KduD rev	GGTGGTGGTGCTCGATTAGCGAGCCAACCAGC
kdgF upstream fwd	GTACCCGGGGATCGCGGAGTTTTTATGGATTTCATCAAG
kdgF upstream rev	ATTAATACTGGGTATCACCACCTCTCTGAAAATATTTAAAGTAG
kdgF downstream fwd	*ATACCCAGTATTAAT*ATGAACTAAAATGGTAGCGCATAAAATG
kdgF downstream rev	CGACTCTAGAGGATCCTTTACCAAACATAGCTTTAGAAC
kdgF flank fwd	TCTCTATGTTGGTGATGGTTCAGGTAGTCC
kdgF flank rev	TCAGAAACAAATGTTCTCGGTTGTTCAAGG
pGEX-*kdgF* fwd	CAGGAAACAGTATTCATGTTTGTATTTAATGAAGATACAGC
pGEX-*kdgF* rev	AGATCGTCAGTCAGTTTACTTTAAAAAATCCTGACGTTGAGG

Utilized restriction sites are shown in bold. Underlining indicates vector-derived sequences used for In-Fusion® cloning. Italics indicate complementary sequence that was used to join the upstream and downstream flanks together.

Supporting Information Figures

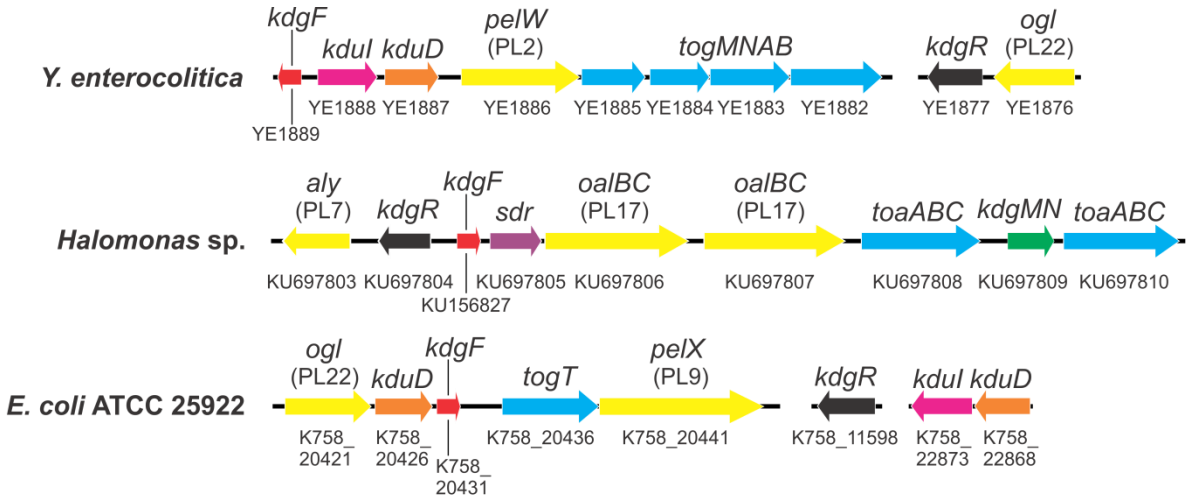

Fig. S1. Polyuronate utilization loci from the pectinolytic bacterium *Y. enterocolitica,* the alginolytic bacterium *Halomonas* sp. and *E. coli* ATCC 25922.

ORFs are color coded according to their predicted function: DKI isomerase (pink), DKII reductase (orange), uronate lyase (yellow), uronate transporter (blue), transcriptional regulator (black), DEH reductase (purple), outer membrane porin (green). Gene name annotations for *Y. enterocolitica* and *E. coli* are taken from Rodionov et al. (23); gene names for *Halomonas* sp., with the exception of *aly*, were assigned according to homology with genes identified in *Vibrio splendidus* (24). PL numbers refer to the family of polysaccharide lyases according to the CAZy database (www.cazy.org). ORFs are to scale within each organism, with locus tags given underneath.

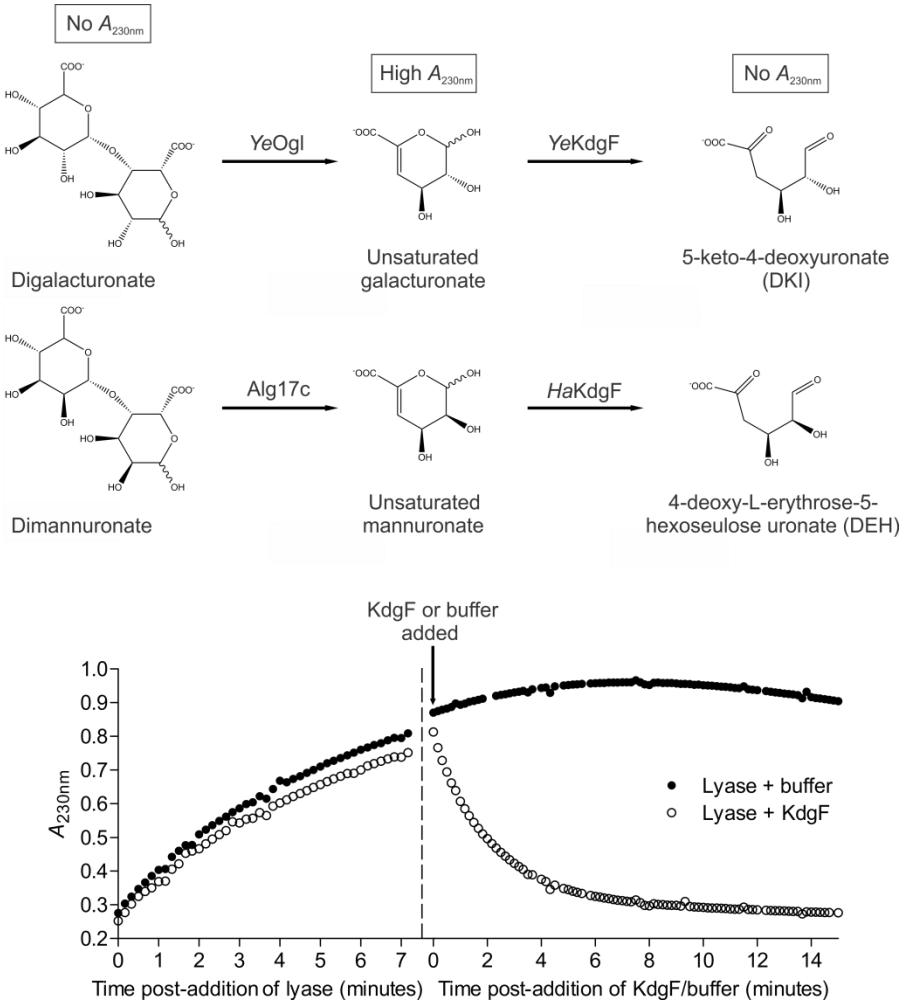

Fig. S2. Coupled assay used for detection of double bond depletion.

Cleavage of a diuronate by a polysaccharide lyase produces a 4,5-unsaturated monouronate, resulting in an increase in absorbance at 230 nm. Subsequent depletion of this double bond – either through spontaneous conversion or the action of KdgF – results in a decrease in absorbance. The data shown are illustrative, and show the effect of the addition of *Ye*Ogl to digalacturonate in two different wells of a microtiter plate (filled circles and open circles), followed by the addition of a buffer blank to one well and 100 nM *Ye*KdgF to the other. The dashed line represents the approx. 10 second gap in data collection while *Ye*KdgF/buffer was added. The significant rate of spontaneous conversion of the unsaturated monouronate means that it cannot be isolated and purified for use as a substrate, and KdgF activity can only be mointored in a coupled assay with a lyase.

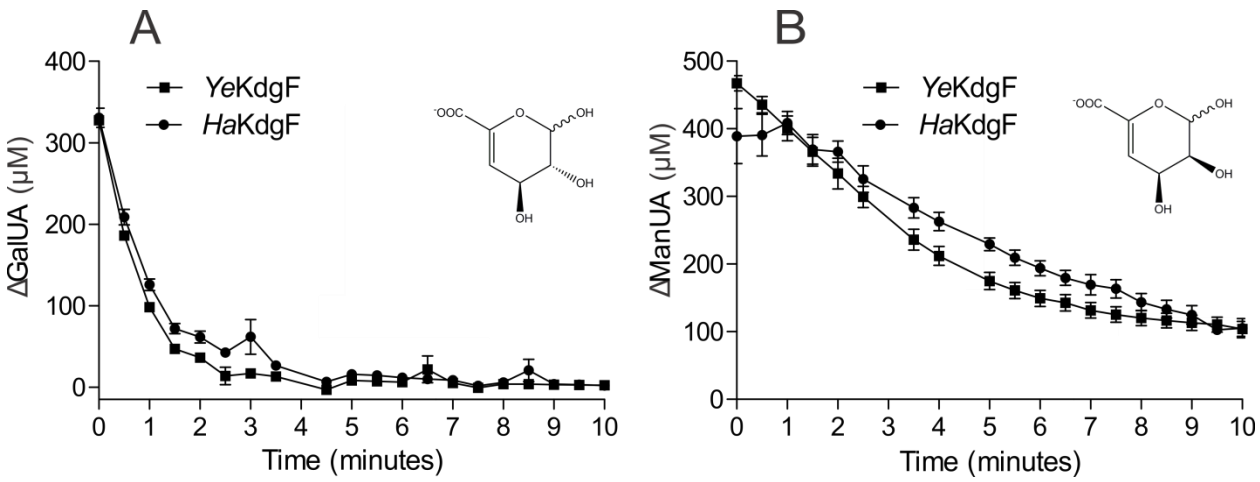

Fig. S3. Substrate specificity of *Ye*KdgF and *Ha*KdgF on unsaturated monouronates. Double bond depletion in unsaturated monouronate in the presence of 1 μM *Ye*KdgF or *Ha*KdgF was followed at 230 nm. (A) Activity of *Ye*KdgF and *Ha*KdgF on unsaturated galacturonate. (B) Activity of *Ye*KdgF and *Ha*KdgF on unsaturated mannuronate. Error bars, where visible, represent the SEM (n=3).

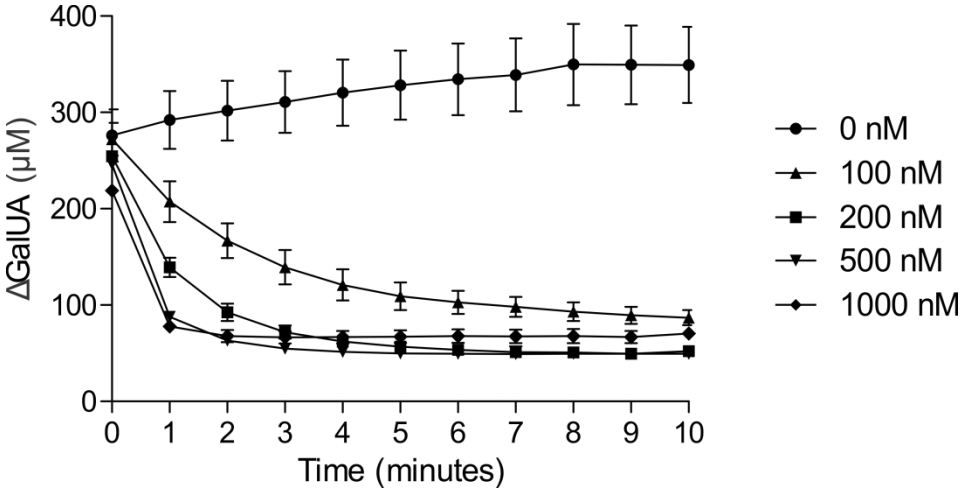

Fig. S4. Concentration-dependent activity of *Ec*KdgF on unsaturated galacturonate. Double bond depletion in unsaturated galacturonate in the presence of increasing concentrations of *Ec*KdgF was followed at 230 nm. Error bars, where visible, represent the SEM (n=3).

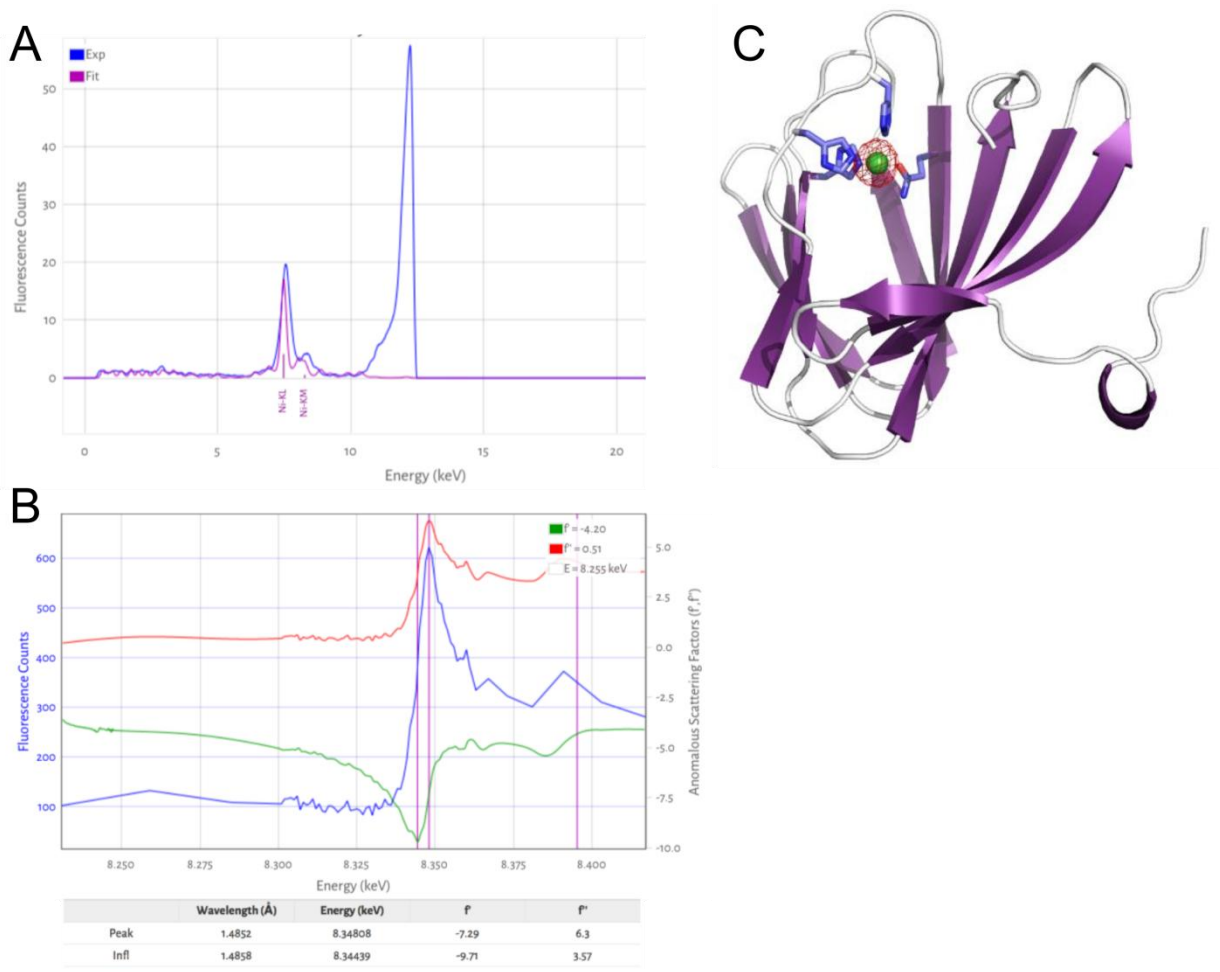

	Wavelength (Å)	Energy (keV)	f'	f''
Peak	1.4852	8.34808	-7.29	6.3
Infl	1.4858	8.34439	-9.71	3.57

Fig. S5. Identification of the metal bound to *Ye*KdgF. (A) X-ray fluorescence excitation of *Ye*KdgF crystals (blue line) overlapped with the theoretical KL and KM edges of Ni (pink line). (B) MAD scan of *Ye*KdgF crystals at the nickel edge. (C) The structure of *Ye*KdgF showing the anomalous difference map contoured at 5σ generated from data collected at the nickel-peak and surrounding the entire monomer. Anomalous difference signal was only detected as overlapping with the modeled metal ion (green sphere).

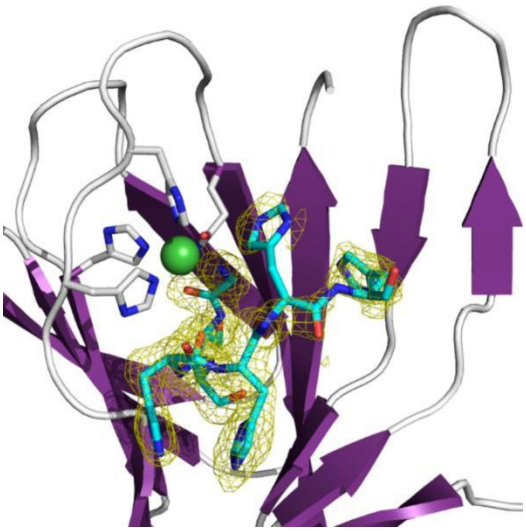

Fig. S6. Structure of *Ye*KdgF in spacegroup $P2_12_12_1$ showing N-terminal 6-histidine tag bound to the metal site. The bound peptide is shown as light blue sticks and its F_o-F_c electron density maps (contoured at 3s) is shown as yellow mesh. Residues coordinating the bound metal atom are shown as grey sticks. A bound metal that was modeled as a Ni^{2+} atom is shown as a green sphere.

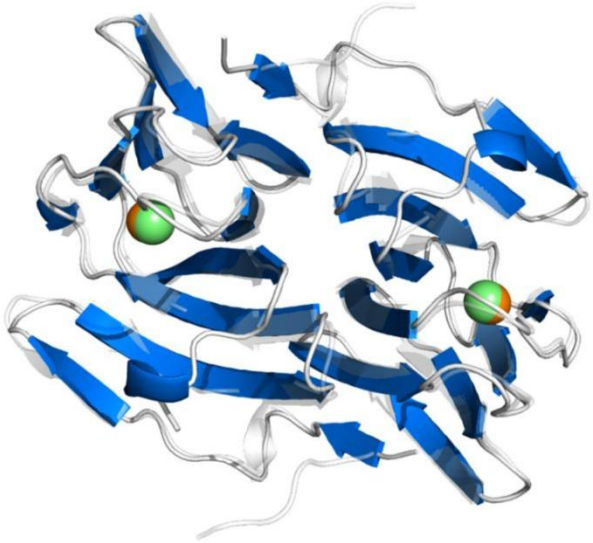

Fig. S7. Structure of *Ha*KdgF. Structure of *Ha*KdgF (blue with green spheres for bound metal atom) determined at 2.35 Å resolution superimposed with the structure of *Ye*KdgF (transparent grey).

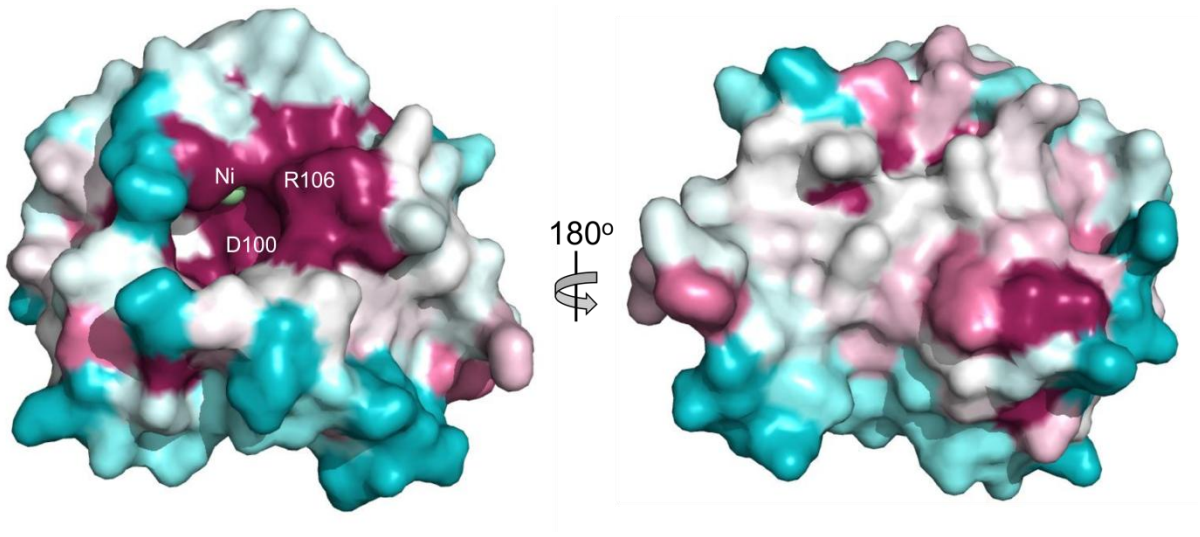

Fig. S8. The conservation of surface exposed residues generated by Consurf analysis and mapped onto the surface of *Ye*KdgF. 400 unique KdgF amino acid sequences were used in the analysis. The positions of the nickel atom (green sphere) and the proposed catalytic residues D100 and R106 are shown for reference. Residue conservation is colored with a gradient from turquoise (variable) through white to dark pink (conserved).

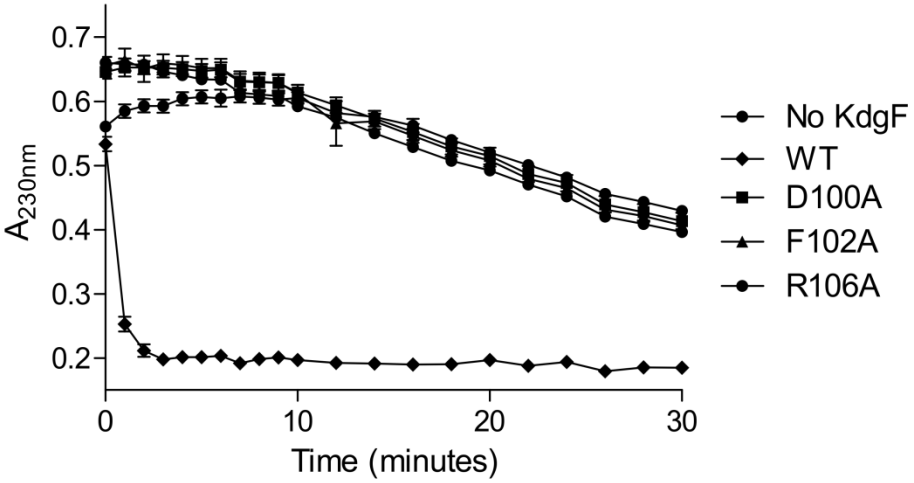

Fig. S9. Inactivity of *Ye*KdgF mutants D100A, F102A and R106A. The double bond depletion activity of *Ye*KdgF mutants at 250 nM on unsaturated galacturonate was followed at A_{230nm} for 30 minutes. Error bars, where visible, represent the SEM (n=4).

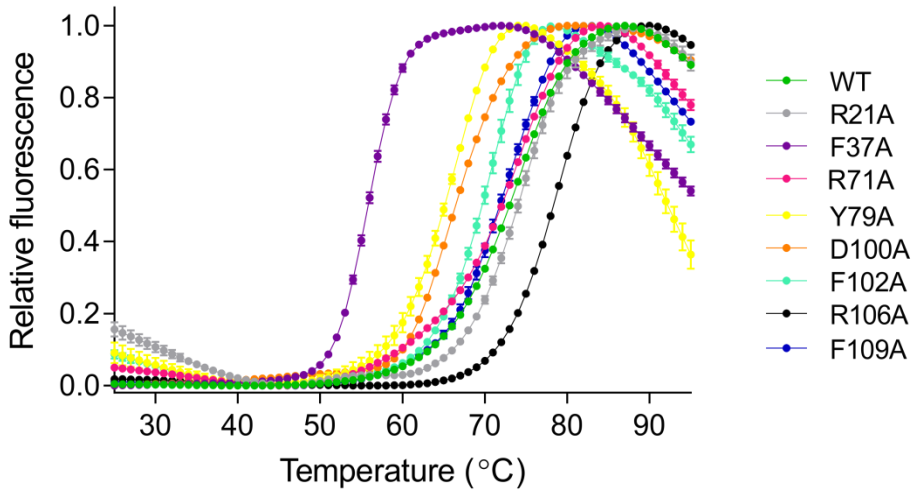

Fig. S10. Thermal unfolding of *Ye*KdgF mutants. The thermal unfolding of wildtype *Ye*KdgF and its mutants was compared using differential scanning fluorimetry. Data are shown relative to the highest fluorescence value for each protein. Error bars, where visible, represent the SEM (n=4).

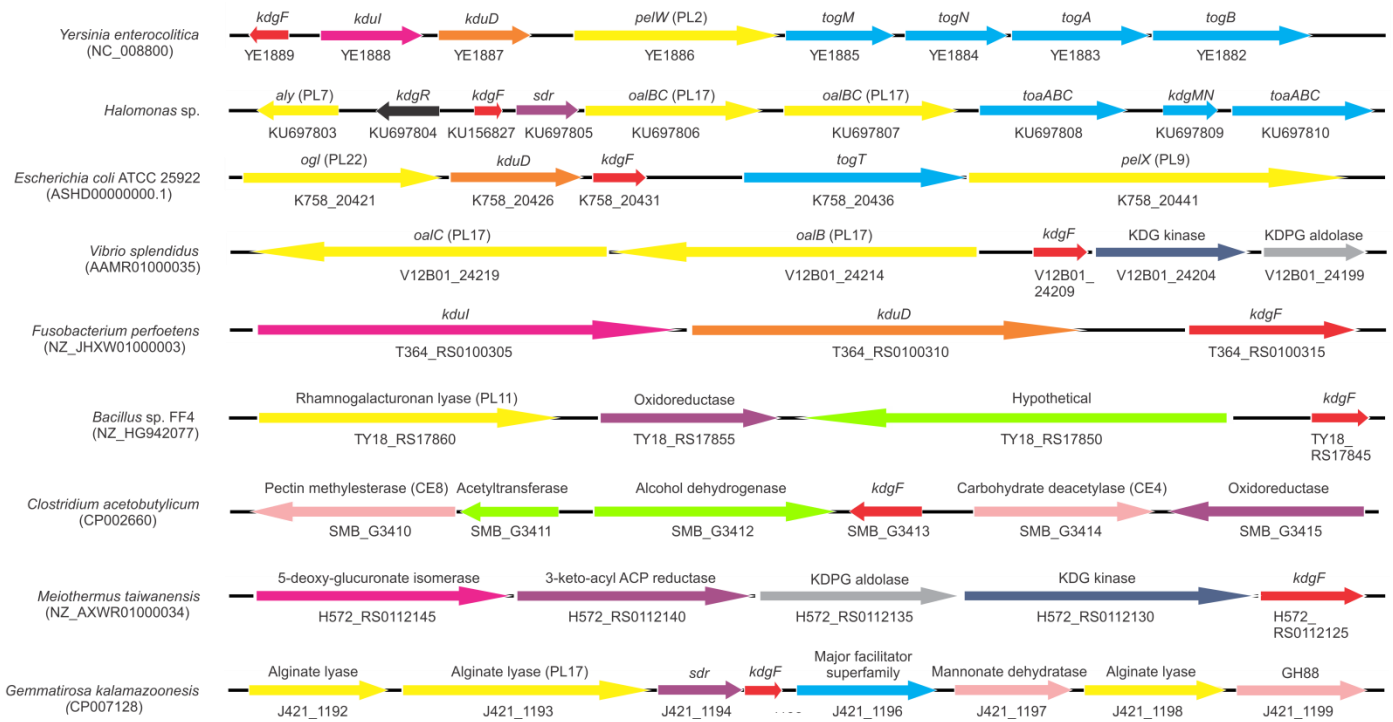

Fig. S11. Genomic context of *kdgF* in diverse bacteria. The genomic context of *kdgF* in bacteria from diverse phyla is shown, specifically when it is associated with other genes involved in carbohydrate metabolism and modification. ORFs are color coded according to their predicted function: KdgF (red), uronate isomerase (fuchsia), sugar dehydrogenase (orange), uronate lyase (yellow), sugar transporter (light blue), transcriptional regulator (black), reductase (purple), KDG kinase (dark blue), KDPG aldolase (grey), other carbohydrate-active enzymes (light pink), hypothetical and other proteins (green). Gene name annotations for *Y. enterocolitica* and *E. coli* are taken from Rodionov et al. (23); gene names for *Halomonas* sp., with the exceptions of *aly* and *sdr*, were assigned according to homology with genes identified in *Vibrio splendidus* by Wargacki et al. (24). PL, GH, CE and GT numbers refer to families of polysaccharide lyases, glycoside hydrolases, carbohydrate esterases and glycosyl transferases, respectively, according to the CAZy database (25); GH88 are a family of unsaturated glucuronyl hydrolases. ORFs are to scale within each organism, with locus tags given underneath.